

Seismicity of the northern part of the Itoigawa-Shizuoka Tectonic Line

Shin'ichi Sakai

Earthquake Research Institute, University of Tokyo, 1-1-1 Yayoi, Bunkyo-ku, Tokyo-to 113-0032, Japan

(Received July 2, 2004; Revised December 14, 2004; Accepted December 24, 2004)

The relationship between recent seismicity and the active fault system was investigated using the precise hypocentral distribution by taking into consideration the heterogeneity of the velocity structure around the northern part of the Itoigawa-Shizuoka Tectonic Line (ISTL), the western boundary of the northern Fossa Magna basin. Since a velocity structure suitable for the ISTL is necessary for precise hypocentral determination, deep seismic reflection and refraction profiling were undertaken in 2002 across the northern part of the ISTL and a reliable velocity model was obtained. The hypocenters were located using the station corrections derived from the velocity model. The obtained hypocenters were found to be distributed in a straight line in an almost north-to-south direction. The hypocenters, whose lower limit was approximately 15 km, were distributed around a vertical plane. The focal mechanism solutions were primarily strike-slip and the direction of their P-axis was NW-SE to WNW-ESE. The fault planes expected from these mechanisms are consistent with the distribution of the hypocenters. However, they are not consistent with the thrust fault planes of previous large earthquakes, which were inferred from the near-surface feature of the active fault system. This suggests that the recent seismicity cannot be attributed to aftershocks of the previous large earthquakes and is not induced by the movement of the active thrust fault.

Key words: Itoigawa-Shizuoka Tectonic Line, seismicity, precise hypocenter.

1. Introduction

The northern part of the Itoigawa-Shizuoka Tectonic Line (ISTL) is the western boundary of the northern Fossa Magna basin and a geological boundary between the old pre-Tertiary basement and the relatively new Neogene sedimentary basin. The ISTL is an active fault system and is recognized as having one of the largest slip rates in the Japanese islands. The slip rate of the Gofukuji Fault, located in the central ISTL, is estimated to be approximately 8.0 mm/yr based on geomorphological and geological studies (Okumura *et al.*, 1994). Across the northern part of the ISTL, GPS measurements indicate horizontal crustal shortening (Sagiya *et al.*, 2002). The present paper investigates the relationship between recent seismicity and the ISTL, which has a large lateral heterogeneity and a large slip rate. The precise hypocentral distribution obtained in consideration of the heterogeneity of the velocity structure may show the current situation of the active fault system and may predict the conditions for the next large earthquake.

2. Seismic observation

The High Sensitivity Seismograph Network (Hi-net) has been deployed by the National Research Institute for Earth Science and Disaster Prevention, and the waveform data are continuously recorded by the Japan Meteorological Agency (JMA). Although the detection capability and determination accuracy of an earthquake have been improved by the new system, hypocenter determination around the ISTL

remains difficult because the ISTL is a major geological boundary and there is a great difference between the velocity structures of the eastern and western sides (Sato *et al.*, 2004). Consequently, errors in hypocentral determinations are large and the distribution of the hypocenters is extended in the vertical direction. A suitable velocity structure is essential to precisely determine the hypocenter in the large lateral heterogeneity. Deep seismic reflection and refraction profiling were undertaken in 2002 across the northern part of the ISTL (Imai *et al.*, 2004; Takeda *et al.*, 2004). In these studies, a suitable velocity structure was obtained and was used for the present hypocentral determination.

3. Hypocenter Distribution

Hypocenters were determined by the maximum-likelihood estimation technique described by Hirata and Matsu'ura (1987). Since the study area has large lateral heterogeneity, three different velocity models were used in the different regions (Fig. 2). The models were derived from previous refraction experiments (Imai *et al.*, 2004; Takeda *et al.*, 2004). Model number 1 has a thick low velocity layer and was adopted for the regions around the ISTL (1, 2, 6 and 8 in Fig. 1); model number 2 was adapted to the region south-east of the ISTL (9 in Fig. 1), which is covered with volcanic products; and model number 3 was adapted for the remaining regions (3, 4, 5 and 7 in Fig. 1).

Hypocenters were located initially using the above three velocity models and arrival times without station corrections. Differences between the observed and estimated travel times were calculated for each station (O-C times) and these were averaged only over the earthquakes that occurred within each of the nine regions shown in Fig. 1. Nine

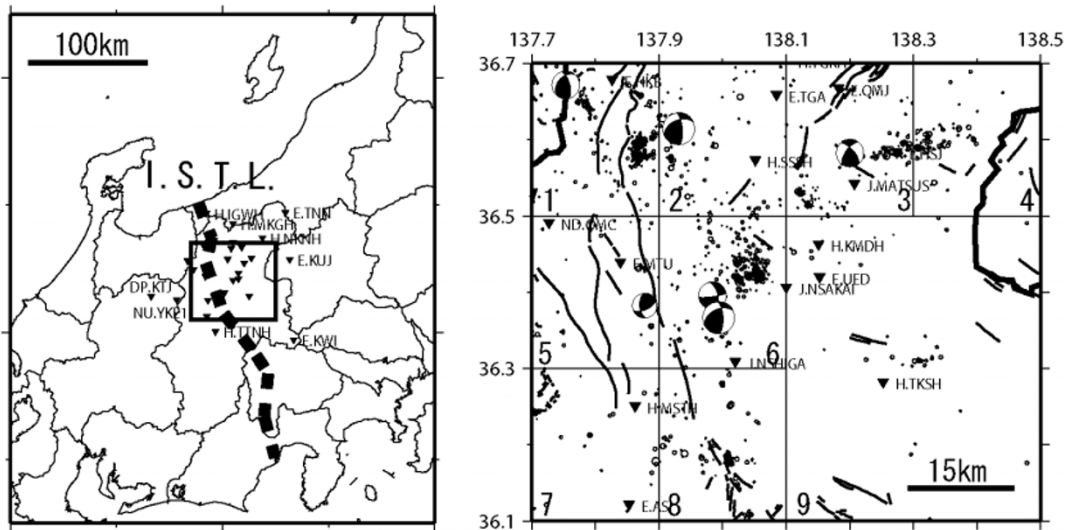


Fig. 1. A location map of the Itoigawa-Shizuoka Tectonic Line (ISTL) is shown in the figure on the left. The square indicates the present study area and the broken line indicates the ISTL. The inverted triangles indicate telemetered seismic stations. Focal mechanism solutions larger than M3.5 in this area are shown in the figure on the right by lower hemisphere projection. The major faults are indicated by a thin line. The hypocenters were determined using different station corrections for the nine regions.

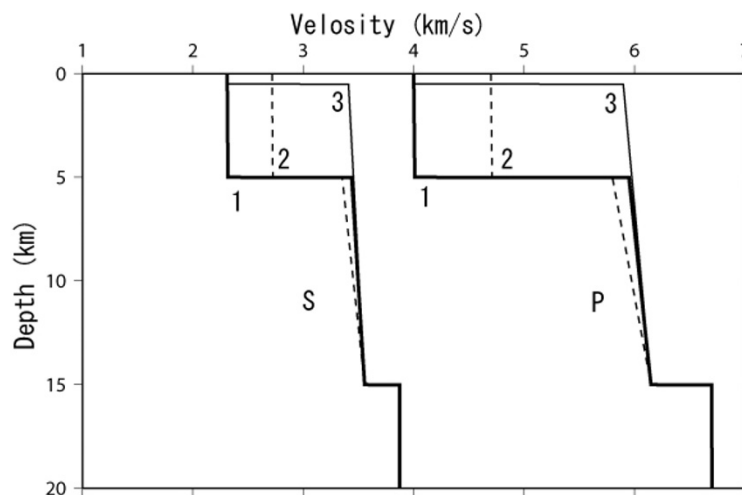


Fig. 2. P-wave and S-wave velocity structure models for hypocenter determination. These models were derived from previous refraction experiments (Imai *et al.*, 2004; Takeda *et al.*, 2004). Model numbers 1 (thick line), 2 (broken line) and 3 (thin line) were adapted for the regions around the ISTL (1, 2, 6 and 8 in Fig. 1), for the south-east region (9) and for the other regions (3, 4, 5 and 7), respectively.

averaged O-C-times were obtained for each station. Next, the hypocenters were located using the averaged O-C times as station-correction values. A new set of averaged O-C times for each station was calculated from the results of the second location procedure. Finally, the new averaged O-C times were added to the previous correction values, and the hypocenters were located again. This relocation process was repeated five times, at which point the final correction values for each station decreased by less than 0.01 s; the obtained final O-C values for each station of the nine regions are listed in Table 1. At the end of this analysis, the averaged O-C times of hypocenter determination decreased from 0.131 s to 0.054 s for P-wave arrival, and from 0.193 s to 0.100 s for S-wave arrival (Table 1). The shape of the curve of frequency became sharp and the deviation is smaller (Fig. 3). Some 1829 hypocenters were selected with the criteria of small spatial errors of less than 1 km in the

horizontal direction and less than 2 km in depth. The period of observation was from 1 January, 2001 to 31 December, 2003.

4. Discussion

The hypocenters around the northern part of the ISTL were distributed in a straight line in an almost north-to-south direction (Fig. 4). The hypocenters were distributed around a vertical plane and their lower limit was approximately 15 km. Although a similar distribution was obtained from the analysis using a uniform one-dimensional velocity structure, the distribution shown in Fig. 4 is clearer than that by the uniform velocity structure. The active fault system around the northern part of the ISTL has a strike in a north-to-south direction. Earthquakes have occurred only in the layer whose velocity is about 6.0 km/s (Fig. 5). Many earthquakes have occurred in the upper crust of the eastern

Table 1. The final station corrections of each station of the nine regions shown in Fig. 1. The upper and lower values for each station are the station corrections of the P- and S-waves, respectively. The numerals attached to the station corrections are the number of earthquakes used for the calculation of the station correction.

	1	2	3	4	5	6	7	8	9									
E.ASI	74	0.11	12	0.42	11	0.139	6	-0.069	50	0.12	296	0.062	68	0.027	172	-0.002	15	-0.054
	6	-0.863	0		2	-0.243	3	-0.702	31	-0.186	64	-0.767	59	-0.513	170	-0.408	8	-0.68
E.HKB	672	0.005	54	-0.06	29	0.092	8	0.264	14	-0.074	71	0.094	5	-0.196	27	0.126	3	0.217
	629	-0.388	45	-0.523	8	0.169	2	-0.03	9	-0.298	36	-0.48	2	-0.968	12	-0.526	0	
E.HSJ	518	-0.318	74	-0.233	258	-0.019	101	0.056	22	0.041	446	-0.092	24	-0.203	105	-0.254	52	-0.005
	201	-0.959	63	-0.914	249	-0.052	98	-0.273	3	-0.259	352	-0.763	0		31	-1.231	44	-0.532
E.KUJ	15	0.252	6	0.114	97	0.498	66	0.217	0		39	0.361	0		11	0.408	9	0.341
	0	0	0	0	6	0.848	22	0.004	0		0	0	0		0	0	0	
E.KWI	5	-0.046	4	-0.069	8	-0.198	5	-0.388	0		47	-0.352	4	-0.041	62	-0.128	21	-0.195
	0	0	0	0	0	0	0	0	0		0	0	0	4	-0.897	6	-1.214	
E.KYJ	757	0.068	69	-0.082	49	-0.22	14	-0.157	63	0.001	357	-0.118	51	-0.025	110	-0.071	9	-0.151
	739	-0.461	48	-0.797	14	-0.723	0		58	-0.133	148	-0.98	37	-0.847	33	-0.874	3	-0.986
E.MTU	692	0.149	58	0.268	52	0.147	17	0.155	61	0.02	414	0.085	54	0.128	123	0.253	12	0.076
	639	-0.309	36	-0.175	10	0.099	0		41	-0.014	283	-0.388	32	-0.317	55	-0.086	3	-0.311
E.OMJ	300	0.522	33	0.47	201	0.035	58	0.187	0		104	0.37	4	0.276	19	0.217	10	0.32
	7	1.039	5	0.712	101	0.416	11	0.29	0		11	0.441	0		0		2	0.469
E.TGA	549	0.333	75	0.198	207	0.126	74	0.345	17	0.901	193	0.466	7	0.666	20	0.413	15	0.311
	76	0.291	41	0.071	61	0.446	19	0.278	2	1.899	9	0.519	0		0		0	
E.TNN	9	-0.004	3	-0.168	15	-0.012	28	-0.312	0		12	0.2	0		2	0.438	0	
	0	0	0	0	3	-0.412	15	-1.067	0		0	0	0		0	0	0	
E.UED	508	-0.065	80	-0.031	238	0.01	97	-0.049	40	0.158	486	0.068	45	0.061	165	0	53	0.09
	198	-0.753	62	-0.609	197	-0.04	72	-0.634	22	0.028	486	-0.445	19	-0.672	93	-0.576	55	-0.321
DP.KTJ	14	0.031	0		2	-0.159	0		8	0.078	12	-0.276	14	-0.15	8	-0.157	0	
	0	0	0	0	0	0	0	0	3	-0.248	0	0	3	-0.968	0	0	0	
H.IGWH	56	-0.215	4	-0.046	5	-0.099	0		0	0	0	0	0	0	0	0	0	
	34	-1.006	3	-0.698	2	-0.239	0		0	0	0	0	0	0	0	0	0	
H.KMDH	69	-0.009	18	-0.039	64	0.047	27	0.004	8	0.082	87	0.111	3	-0.053	13	-0.018	17	0.023
	25	-0.623	15	-0.691	58	0.042	26	-0.504	6	0.025	82	-0.436	0		3	-0.666	17	-0.52
H.MKGH	37	0.079	7	0.117	12	0.162	2	0.188	0		7	0.629	0		0	0	0	
	16	-0.378	2	-0.314	3	0.418	2	-0.119	0		0	0	0	0	0	0	0	
H.MSTH	50	0.131	10	0.513	6	0.181	0		14	0.055	99	0.1	28	0.059	114	0.089	12	0.053
	26	-0.504	3	0.118	0	0	0		11	-0.003	50	-0.562	28	-0.395	97	-0.362	5	-0.614
H.NKNH	33	-0.187	5	-0.114	54	-0.189	45	-0.255	0		26	-0.04	0		0	10	-0.175	
	2	-0.668	0		39	-0.491	39	-0.931	0		5	-0.899	0		0	4	-0.936	
H.SSSH	46	0.674	13	0.351	23	0.27	0		2	0.855	18	0.478	0		0	3	0.351	
	21	0.905	7	0.291	8	0.63	0		0	6	0.514	0	0	0	0	0		
H.TGKH	30	0.433	12	0.328	55	0.378	10	0.636	3	1.132	28	0.865	0		0	6	0.619	
	12	0.351	4	0.301	27	0.862	5	0.953	0	0	0	0	0	0	2	0.76		
H.TKSH	23	-0.025	12	0.073	49	0.253	15	0.241	6	0.029	111	0.036	9	-0.087	106	0.024	27	0.106
	8	-0.696	7	-0.58	23	0.291	7	-0.134	3	-0.143	96	-0.609	2	-1.029	96	-0.5	25	-0.304
H.TTNH	21	0.104	3	0.495	6	-0.036	2	-0.189	5	0.122	30	0.021	26	0.002	110	0.081	4	-0.078
	3	-0.911	0	0	0	0	0	0	3	-0.198	8	-0.797	11	-0.778	100	-0.416	0	
ND.OMC	688	-0.018	42	-0.074	55	-0.195	14	-0.099	53	-0.059	367	-0.16	42	-0.101	108	-0.064	11	-0.197
	604	-0.552	25	-0.727	14	-0.637	0		38	-0.117	211	-0.939	26	-0.783	17	-0.792	4	-0.981
NU.YKE1	42	-0.006	9	0.124	3	-0.223	4	-0.258	45	0.05	80	-0.156	60	0.033	86	-0.139	0	
	0	0	0	0	0	0	0	0	33	-0.192	8	-1.259	47	-0.526	20	-1.067	0	
J.MATSUS	605	-0.215	84	-0.149	258	-0.016	101	-0.065	33	0.108	481	-0.051	31	-0.089	126	-0.2	54	-0.07
	238	-0.821	57	-0.762	233	-0.026	78	-0.517	4	-0.241	366	-0.631	6	-0.842	25	-0.94	45	-0.577
J.NSAKAI	5	0.014	0		6	0.104	8	0.111	6	0.043	29	0.069	0		3	0.061	2	-0.057
	3	-0.438	0		5	0.162	2	-0.718	5	0.217	28	-0.499	0		3	-0.255	2	-0.532
J.NSHIGA	0	0	0		3	-0.064	0		4	0.199	66	-0.034	2	0.257	17	0.123	4	-0.193
	0	0	0		3	-0.104	0		4	0.439	57	-0.58	2	0.204	15	-0.089	3	-0.693

side of the ISTL.

The hypocenter distribution is not consistent with the fault plane of past thrust earthquakes, which is inferred from the near-surface feature of the active fault system. The active fault system is estimated by some geological studies and seismic experiments (Sato *et al.*, 2004; Imai *et al.*, 2004) to consist of east-dipping low-angle thrust faults with an azimuth of almost north-to-south in direction. The distribution of hypocenters around the northern part of the ISTL is a straight north-to-south and is located slightly eastward of the active fault system. Both distributions show essentially the same direction, suggesting the possibility that movement of the active fault induced the recent earthquake activity. However, the distribution of hypocenters is not

east-dipping, but vertical. The focal mechanism solutions are mainly strike-slip and the direction of the P-axis is NW-SE or WNW-ESE (Fig. 1). The fault planes expected from these mechanisms are consistent with the obtained distribution of hypocenters, and there is a clear distinction between the distribution of recent hypocenters and the geometry of the active fault system.

This distinction may originate in the difference in timescale. The present microearthquakes have been observed for only three years at most. The active fault system expresses the cumulative deformations of some million years. The recent earthquakes in this area reflect only the recent stress field and/or the easy-rupture zone. The fact that the distribution of the hypocenters forms a straight line

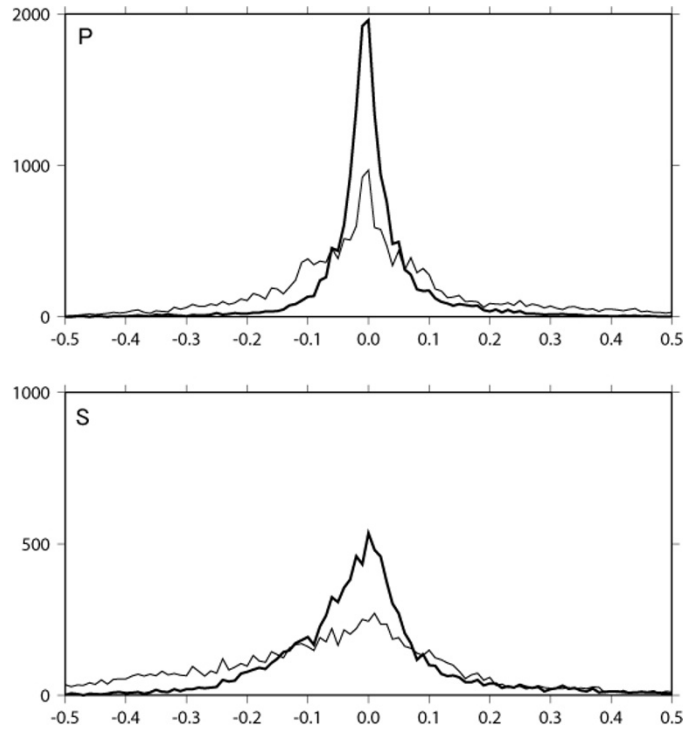


Fig. 3. The frequencies of the residuals for all stations are shown. Thin and thick lines represent the residuals of the initial and final frequencies, respectively. At the end of this analysis, the averaged residual of hypocenter determination decreased from 0.131 to 0.054 s for P-wave arrival and from 0.193 to 0.100 s for S-wave arrival. Note that the shape of the curve of frequency becomes sharp.

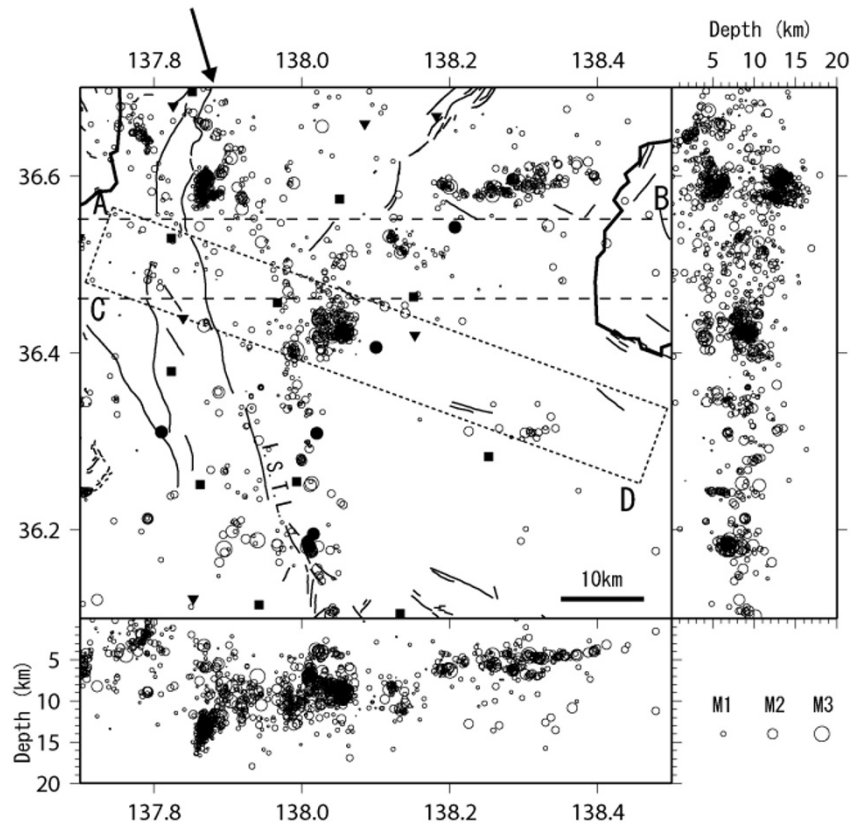


Fig. 4. Hypocenter distribution was obtained taking into consideration the heterogeneity of the velocity structure in the present study, which was carried out from 1 January, 2001 to 31 December, 2003. The solid circles, the solid inverted triangles and the solid squares indicate the positions of the seismic stations of the Japan Meteorological Agency, the Earthquake Research Institute and the National Research Institute for Earth Science and Disaster Prevention, respectively. The two squares with broken lines indicate the area of the profile in Fig. 5. The bottom area shows the E-W cross-section and the right shows the N-S cross-section. Hypocenters with an error of less than 1 km for the horizontal direction and less than 2 km in depth are plotted. In the horizontal section, the arrowed line indicates the distribution of hypocenters in a straight line in an approximately north-to-south direction. This distribution also exists in areas other than the ISTL.

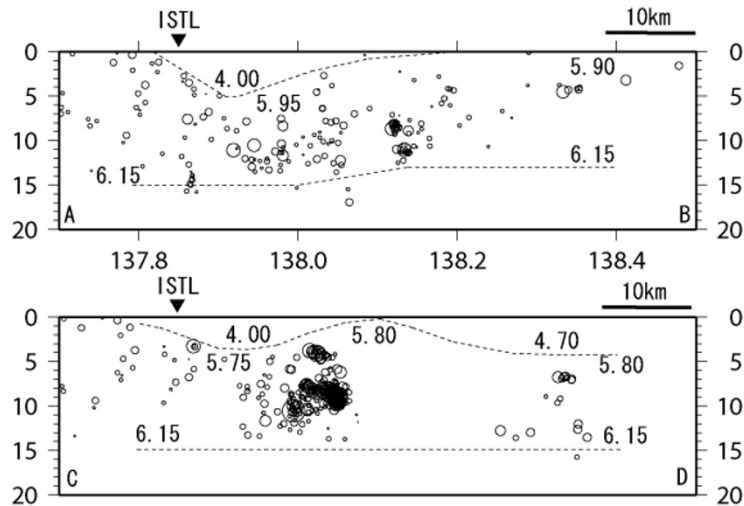


Fig. 5. Profile of the hypocenter distributions obtained taking into consideration the heterogeneity of the velocity structure. The top profile is the experiment line in the east-to-west direction (Takeda *et al.*, 2004) and the bottom profile is the experiment line in the direction of WNW-ESE (Imai *et al.*, 2004). The range of the profiles is shown by the two squares in Fig. 4. The simplified models of the velocity structures are indicated by the broken line and the value of the P-wave velocity. The solid triangle indicates the position of the ISTL. Earthquakes have occurred only in the layer whose P-wave velocity is about 6.0 km/s. Some earthquakes have occurred on the eastern side of the ISTL, and the distributions do not form a thrust fault plane of the previous large thrust earthquakes, which is expected from the near-surface feature of the active fault system.

suggests that recent stress is concentrated on this line and/or that the weak zone is locating along this line. It appears that the hypocenters do not express a fault plane which will be ruptured by a large earthquake in the near future or a fault plane which ruptured in the past.

Given that tectonic stress accumulation and crustal shortening always exist, the cumulative stress must necessarily be released from time to time. Usually, relatively small earthquakes with a strike-slip type occur in the upper crust in order to release the stress. However, it may be insufficient to release the stress only by these earthquakes. The remaining stress may thus be released by a large thrust earthquake, possibly when the rate of tectonic stress accumulation episodically increased and/or the stress exceeded the fault strength. This may be an explanation of the distinction between the distribution of recent earthquakes and the thrust faults identified around the northern part of the ISTL.

5. Conclusion

The relationship between recent seismicity and the ISTL, which has a large lateral heterogeneity, was investigated using the precise hypocentral distribution obtained taking into consideration the heterogeneity of the velocity structure. The precise hypocenters were determined by the velocity structure derived from the deep seismic reflection and refraction profiling which was carried out in 2002. The obtained hypocenters were found to be distributed in a straight north-to-south line. They were distributed around a vertical plane and had a lower limit of approximately 15 km. The focal mechanisms were primarily strike-slip with a P-axis in the NW-SE or WNW-ESE direction. The fault planes expected from these mechanisms are consistent with the distribution of hypocenters, however, they are not consistent with the plane of the thrust fault of previous large earthquakes, which was inferred from the near-surface feature of the active fault system. This suggests that the recent seismicity is

not related to aftershocks of previous large earthquakes or the displacement of the active thrust fault.

Acknowledgments. The author would like to offer special thanks to Mr. M. Kobayashi, Mr. S. Hashimoto and Mr. T. Haneda for their help with the temporary observations. He gratefully acknowledges helpful discussions with Dr. H. Sato, Dr. T. Iwasaki, Ms. T. Imai and Dr. T. Takeda. Comments by Dr. K. Katsumata and an anonymous reviewer helped him improve the manuscript. He also would like to offer special thanks to Dr. Y. Iio for his advice, his help, and encouragement. This study is a part of the research project on “Slip and Flow Processes in and below the Seismogenic Region”.

References

- Hirata, N. and M. Matsu'ura, Maximum-likelihood estimation of hypocenter with origin time eliminated using nonlinear inversion technique, *Phys. Earth Planet. Inter.*, **47**, 50–61, 1987.
- Imai, T., T. Iwasaki, T. Takeda, T. Kawanaka and H. Sato, Detailed upper crustal structure across the Itoigawa-Shizuoka Tectonic Line from the 2002 seismic expedition, Proceedings of the 2nd International Symposium on Slip and Flow Process in and below the Seismogenic Region, 2004.
- Okumura, K., K. Shimokawa, H. Yamazaki and E. Tsukuda, Recent surface faulting events along the middle section of the Itoigawa-Shizuoka Tectonic Line—trenching survey of the Gofukuji Fault near Matsumoto, central Japan—, *Zisin*, **46**, 425–438, 1994 (in Japanese with English abstract).
- Sagiya, T., T. Nishimura, Y. Iio and T. Tada, Crustal deformation around the northern and central Itoigawa-Shizuoka Tectonic Line, *Earth Planets Space*, **54**, 1059–1063, 2002.
- Sato, H., T. Iwasaki, S. Kawasaki, Y. Ikeda, N. Matsuta, T. Takeda, N. Hirata and T. Kawanaka, Formation and shortening deformation of a back-arc rift basin revealed by deep seismic profiling across the Itoigawa-Shizuoka Tectonic Line active fault system, Central Japan, *Tectonophysics*, 2004 (in press).
- Takeda, T., H. Sato, T. Iwasaki, N. Matsuta, S. Sakai, T. Iidaka and A. Kato, Crustal structure in the northern Fossa Magna region, central Japan, from refraction/wide-angle reflection data, *Earth Planets Space*, **56**, this issue, 1295–1301, 2004.